

5) due to the role of RC, as previously discussed. In a tree-level calculation $\Omega_\chi h^2$ at the representative point of fig. 5 would look as shown in fig. 8; here one notices that above the threshold for $\chi\chi \rightarrow hA$ the values of $\Omega_\chi h^2$ are about one order of magnitude smaller than in fig. 5.

We note that in those figures $\Omega_\chi h^2 < 1$ almost everywhere. More generally, in the region of M_2 , μ explored in this paper, overclosure occurs only for small m_χ , mainly in regions already excluded by present LEP experimental searches.

For the computations of the event rates relevant to direct and indirect searches we need to determine the local (solar neighbourhood) value of the neutralino density ρ_χ . In those regions of the explored range of m_χ where the value of $\Omega_\chi h^2$ is ≥ 0.05 , and then consistent with the value of the local density ρ_1 , we take $\rho_\chi = \rho_1$.

Otherwise, when $\Omega_\chi h^2 < 0.05$, one cannot maintain that the neutralino constitutes the entire DM; ρ_χ must then be rescaled with respect to ρ_1 [5,16]. Thus here, whenever $\Omega_\chi h^2 < 0.05$, we rescale as follows:

$$\rho_\chi = \frac{\Omega_\chi h^2}{0.05} \rho_1. \quad (3.6)$$

Note that in the regions where rescaling occurs one has

$$\rho_\chi \propto \Omega_\chi h^2 \propto \langle \sigma_{\text{ann}} v \rangle_{\text{int}}^{-1}. \quad (3)$$

As we shall see, this proportionality has markable implications on the theoretical predictions for direct and indirect detection.

4. Direct detection

The direct search for the neutralino DM based on the measurement of the effects induced in appropriate detectors by the neutralino-nucleus elastic scattering.

The event rate per nucleus is given by

$$R = \frac{v_\chi \rho_\chi \sigma}{m_\chi}, \quad (4)$$

where σ is the elastic cross-section and v_χ is the neutralino average velocity.

In order to evaluate σ the following process have to be considered: (1) Z-exchange: this provides a spin-dependent cross-section for higgsino (the coherent part is missing due to the Majorana character of the neutralino); (2) squark-exchange

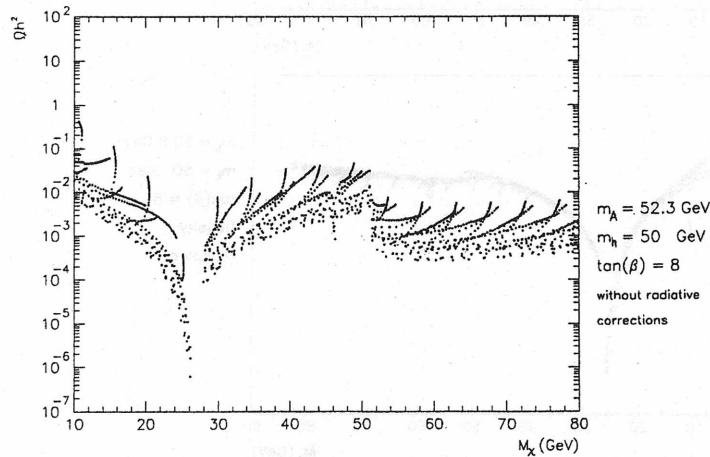


Fig. 8. An example of $\Omega_\chi h^2$ as a function of the neutralino mass m_χ computed at tree level. Here $\tan \beta = 8$, $m_h = 50$ GeV, $m_A = 52.3$ GeV (to be compared with fig. 5 where RC are included).

this gives a coherent contribution for \tilde{Z} -higgsino mixture as well as an incoherent cross-section mainly for gauginos; (3) Higgs boson-exchange: this term gives a coherent cross-section for \tilde{Z} -higgsino mixture.

For the nuclei used in present detectors (Ge, NaI, Si) the coherent scattering is by far dominant. The squark-exchange contribution can be safely neglected compared to the Higgs-exchange one if we take for both the Higgs and the squark masses values close to the present experimental lower bounds, $m_h = 50$ GeV, $m_{\tilde{q}} = 150$ GeV; indeed, corrections due to inclusion of squark-exchange diagram are $(m_h/m_{\tilde{q}})^2 \approx 0.1$ in this case.

As far as the Higgs-nucleon coupling is con-

cerned, we employ here the values reported in ref. [17]. These values differ somewhat from those given by other authors. The effects of this theoretical uncertainty on the event rate are discussed in ref. [3].

As for the spin-dependent cross-sections, the sole Z-exchange contribution may be retained, due to the above lower limit on $m_{\tilde{q}}$.

By way of example the rate for χ -Ge scattering is given for the two cases of non-rescaled (fig. 9a) and rescaled (fig. 9b) ρ_χ . By comparing the two yields one notices two main features in the rescaled case: (i) the spread at a given value of m_χ shrinks greatly and, (ii) the overall value of the yield is dramatically reduced.

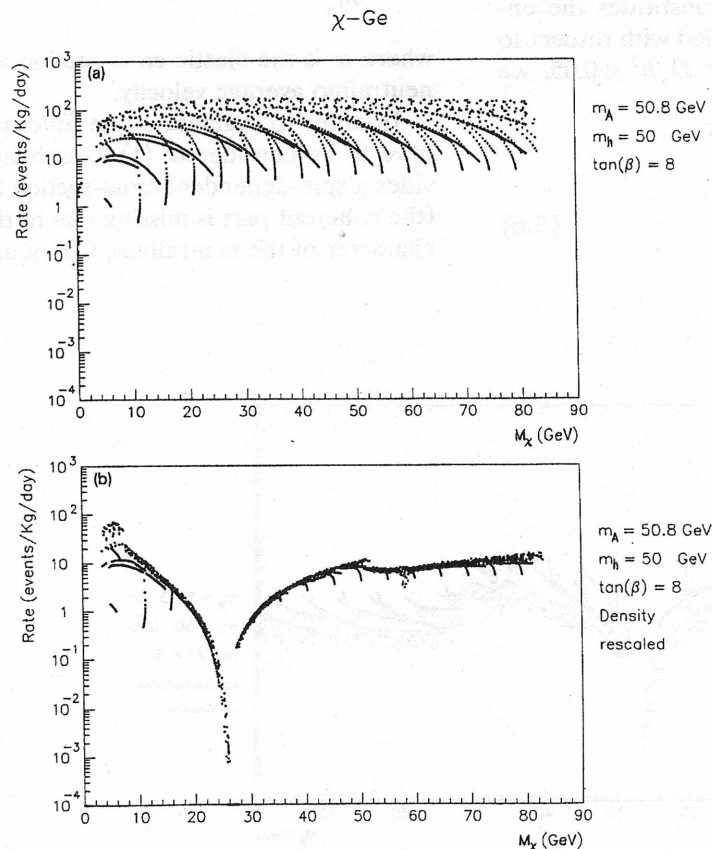


Fig. 9. Rate for χ -Ge scattering events/(Kg day) for $\tan \beta = 8$, $m_h = 50$ GeV, $m_A = 50.8$ GeV. (a) $\rho_\chi = \rho_1$; (b) ρ_χ has been rescaled.

The reason for (i) is that, because of the rescaling, the rate is proportional to $\sigma/\langle\sigma_{\text{ann}}\rangle_{\text{int}}$ (see eq.(3.7)). At low m_χ , when only the ff annihilation channel is open, the cross-section σ_{ann} is dominated by exchange of the pseudoscalar A whereas σ is dominated by the h-exchange diagram. Now, the amplitude for $\chi\chi \rightarrow A \rightarrow q\bar{q}$ depends on the parameters M_2 and μ only through m_χ and the factor

$$F_A \equiv a_2(-a_3 \sin \beta + a_4 \cos \beta) \times \begin{cases} 1/\tan \beta, & \text{for up-type quarks,} \\ \tan \beta, & \text{for down-type quarks,} \end{cases} \quad (4.2)$$

whereas the amplitude for $\chi q \rightarrow \chi q$ (with an exchanged h in t channel) has a dependence through m_χ and

$$F_h \equiv a_2(a_3 \sin \alpha + a_4 \cos \alpha) \times \begin{cases} \cos \alpha/\sin \beta, & \text{for up-type quarks,} \\ -\sin \alpha/\cos \beta, & \text{for down-type quarks.} \end{cases} \quad (4.3)$$

Since, by including RC to Higgs masses, one has, for $\tan \beta \geq 2-3$, $\alpha \approx -\beta$, it also follows that

$$F_A \approx F_h, \quad (4.4)$$

except for very small values of $\tan \beta$. If we further notice that in this ff annihilation $q\bar{q}$ (with heavy q) final states dominate, we can conclude that the dependence of $\sigma/\langle\sigma_{\text{ann}}\rangle_{\text{int}}$ on M_2 and μ is strongly attenuated. We wish to stress that the property for the rate of being largely independent on M_2 and μ follows from the combined effects of the rescaling and of the inclusion of RC to Higgs masses. When the process $\chi\chi \rightarrow hA$ opens the effect becomes less pronounced.

The theoretical prediction at point(ii) shows that a rather high sensitivity is needed in the experimental search. Detailed quantitative comparisons between theory and data have been presented in [3,18] where it is seen that the sensitivity in the present direct measurements is not yet sufficient to place constraints over the neutralino parameters. In ref. [18] the outlooks and perspectives

of direct neutralino search are also discussed.

5. Indirect detection: results and conclusions

Relic neutralinos with local density ρ_χ crossing the Sun or the Earth may lose energy by elastic scattering on the nuclei of the celestial body and become gravitationally trapped. So the Sun and the Earth keep accumulating neutralinos; the density grows with time, and also the rate for χ annihilation increases until it matches the capture rate. The subsequent pair annihilation of the accumulated neutralinos may generate a steady flux of neutrinos from the celestial bodies.

The most accurate study of the capture rate has been performed by Gould [19]. A compact formula for the capture rate is [5,20]

$$C = \frac{\rho_\chi}{v_\chi} \sum_i \frac{\sigma_i}{m_\chi m_i} (M_B f_i) \langle v_{\text{esc}}^2 \rangle_i X_i, \quad (5.1)$$

where σ_i is elastic χ cross-section off nucleus i , m_i is the mass of the element i in the macroscopic body of mass M_B , $\langle v_{\text{esc}}^2 \rangle_i$ is the square escape velocity averaged over the distribution of the element i , X_i is a factor which takes into account further neutralino-nucleus kinematical effects.

The slowing down of χ by elastic scattering is most efficient when m_χ is equal to the mass of some scatterer nucleus inside the celestial body. The presence of heavy nuclei in the Earth makes it very efficient in capturing χ 's in our m_χ range.

For capture when $m_\chi \gg m_w$ the Earth loses efficiency while the Sun, in spite of the smaller nuclei mass, is still effective because of its much larger escape velocity. (For a discussion of indirect detection in this high m_χ regime see ref. [21]).

In the region of parameters in which we are interested here one can assume that both in the Sun and in the Earth equilibrium between capture and annihilation rates has been reached; this is certainly true for the Sun and marginally so also for the Earth.

So at equilibrium $\Gamma_{\text{ann}} = \frac{1}{2}C$ and the flux of neutrinos at a distance d from the annihilation region is given by

$$\frac{dN_\nu}{dE_\nu} = \frac{\Gamma_{\text{ann}}}{4\pi d^2} \sum_f B_f \frac{dN_{f,\nu}}{dE_\nu} \quad (5.2)$$

Here $dN_{f,\nu}/dE_\nu$ denotes the differential distribution of the neutrinos generated by the semileptonic decays of the fermions produced by $\chi\chi$ annihilations; B_f are the relevant branching ratios. The ν_μ 's may then convert into muons into the Earth and thus generate a signal of muons which would cross a neutrino telescope upwardly.

From (5.2) the estimate of the final upgoing muon flux can be obtained by well established computations (see, for instance, ref. [22] and ref. [3]).

We summarize in some figures a sample of our computations for the upgoing muon yield in the case of the Earth and of the Sun. The representative points are selected as before. The neutralino local density is rescaled as explained when $\Omega_\chi h^2 < 0.05$. Events are referred to a detector of area \times time of $10^5 \text{ m}^2 \text{ year}$; the muon threshold energy has been set at 2 GeV.

For the Earth a half aperture of 30° has been used. The background of upgoing muons due to

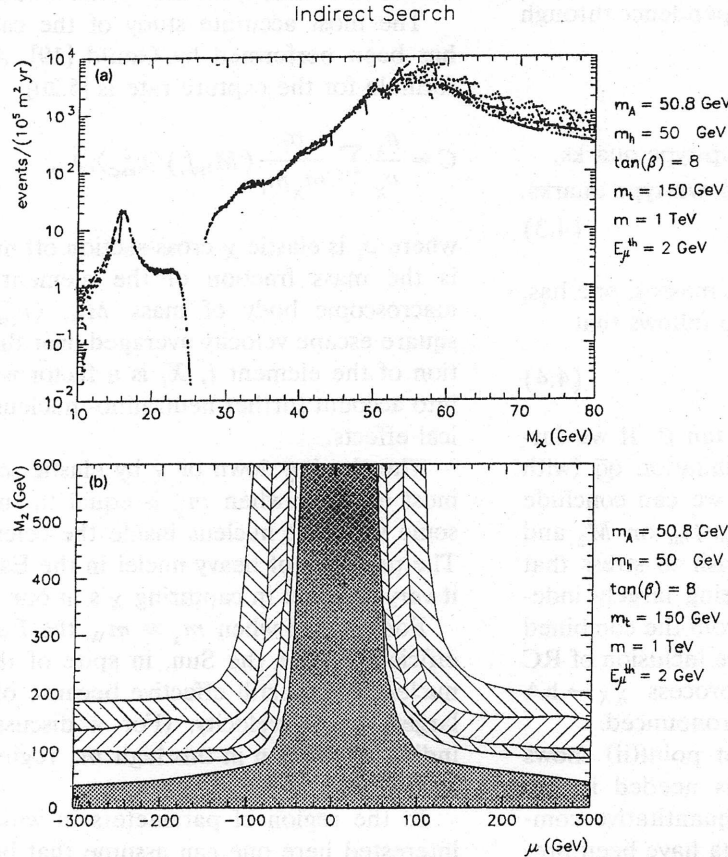


Fig. 10. Indirect detection of neutralinos ($\chi\chi$ annihilation in the Earth): rates of upgoing muons in a detector of area 10^5 m^2 . Half aperture is 30° . ρ_χ is rescaled. Parameters are: $\tan \beta = 8$, $m_h = 50$ GeV, $m_A = 50.8$ GeV. The threshold for muons is 2 GeV. (a) Upgoing-muon rate per year as a function of m_χ ; (b) the upper-left to lower-right dashed plus the inner lower-left to upper right dashed regions represent the domain in the parameter space that can be covered at 4σ in 3 years. The inner dashed area is the region presently excluded by the upper limit [24]. The dotted domain denotes the area excluded by LEP-CDF.

atmospheric neutrinos is $\Phi = 2.5 \times 10^{-13} \text{ cm}^{-2} \text{ s}^{-1} \text{ sr}^{-1}$ [23], which translates into about 6500 events/year in a 10^5 m^2 detector.

Figure 10a shows the event rate for the Earth as a function of m_χ at $m_h = 50 \text{ GeV}$ and $\tan \beta = 8$. The yield follows the general trend of $\Omega_\chi h^2$, in particular the dip in the intensity of the signal is the direct consequence of the enhancement in the annihilation when $m_\chi = \frac{1}{2}m_A$ and of the ensuing depletion of $\Omega_\chi h^2$. In this scatter plot the reduced spread, which is particularly pronounced below the threshold for hA channel in annihilation, is due to the properties already discussed in connection with the direct measurements.

In fig. 10b we represent the region in param-

eter space that can be covered at 4σ in a period 3 years in a detector of 10^5 m^2 . We stress that this search could cover virtually all of the parameter space below the kinematical limit $m_\chi < M$ (notice that the central dotted region is excluded by accelerator searches). The inner dashed arc shows the region presently excluded by the upper limit established at Kamiokande [24] $\Phi \leq 4.0 \cdot 10^{-14} \text{ cm}^2 \text{ s}^{-1}$ (90% C.L.).

Figure 11a shows the yield from the Earth when $m_h = 80 \text{ GeV}$ and $\tan \beta = 8$. The region that can be explored at 4σ over the background is shown in fig. 11b.

It is remarkable that in both cases shown above the region that can be explored in 3 years

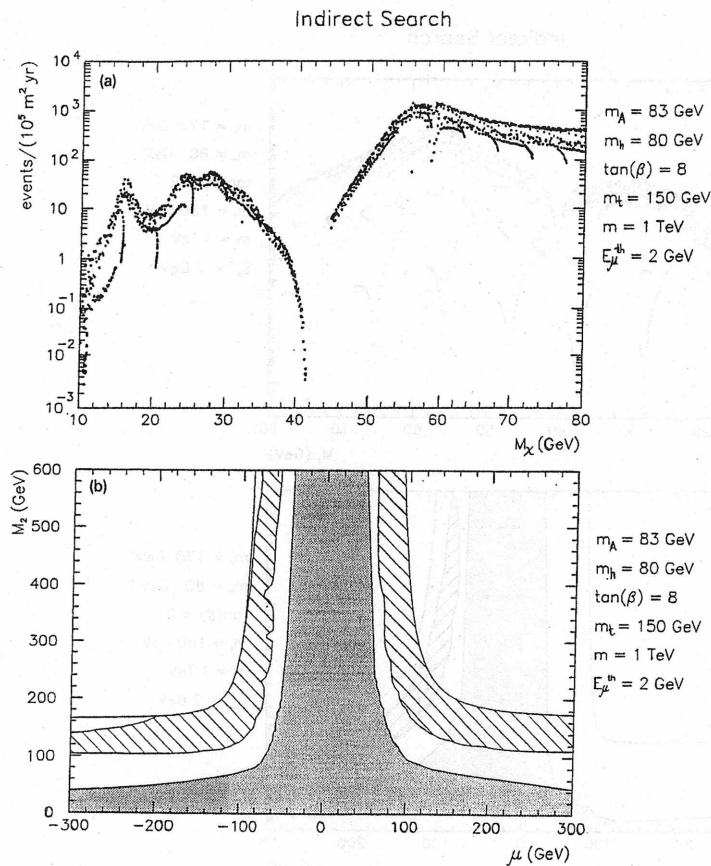


Figure 11b

Fig. 11. Same as in fig. 10 with $\tan \beta = 8$, $m_h = 80 \text{ GeV}$, $m_A = 83 \text{ GeV}$. (a) upgoing-muon rate per year as a function of m_χ ; (b) the dashed region is the domain in the parameter space that can be covered at 4σ in 3 years.

complementary to present accelerator searches and includes domains that will not be reached by future searches at LEP II.

The case $m_h = 80$ GeV and $\tan \beta = 2$ is less favourable, essentially due to the low value of $\tan \beta$. We see an ample spread of the yield as function of the parameters in fig. 12a. The lower overall level of the rate entails a reduced possibility for exploring a region at 4σ over the background, as pictured in fig. 12b.

Let us now discuss the yield from the Sun. The signal and the background have been computed for a half aperture of 25° and an efficiency factor of 0.15. The background is 670 events/ 10^5 m^2 /year. The yields are reproduced in fig. 13. Again typically for a given m_χ the yield shows a weak dependence on M_2 and μ for $\tan \beta = 8$,

while the dependence on these parameters is strong for $\tan \beta = 2$.

The Kamiokande upper limit for the flux from the Sun is [24] $\Phi < 6.6 \times 10^{-14}$ $\text{cm}^{-2} \text{s}^{-1}$ (90% C.L.). This limit corresponds to a yield of about 310 muons/year in 10^5 m^2 ; the fluxes shown in fig. 13 are too low for providing constraints from this experimental bound.

We see from our results that, in the m_χ range considered here, the detection of the signal from the Sun (which is otherwise important for its signature over the background) would require a detector of an area larger than 10^5 m^2 , while the signal from the Earth can be well detected in a few years of operation with a neutrino telescope of area 10^5 m^2 in large regions of parameters if $m_h < 100$ GeV.

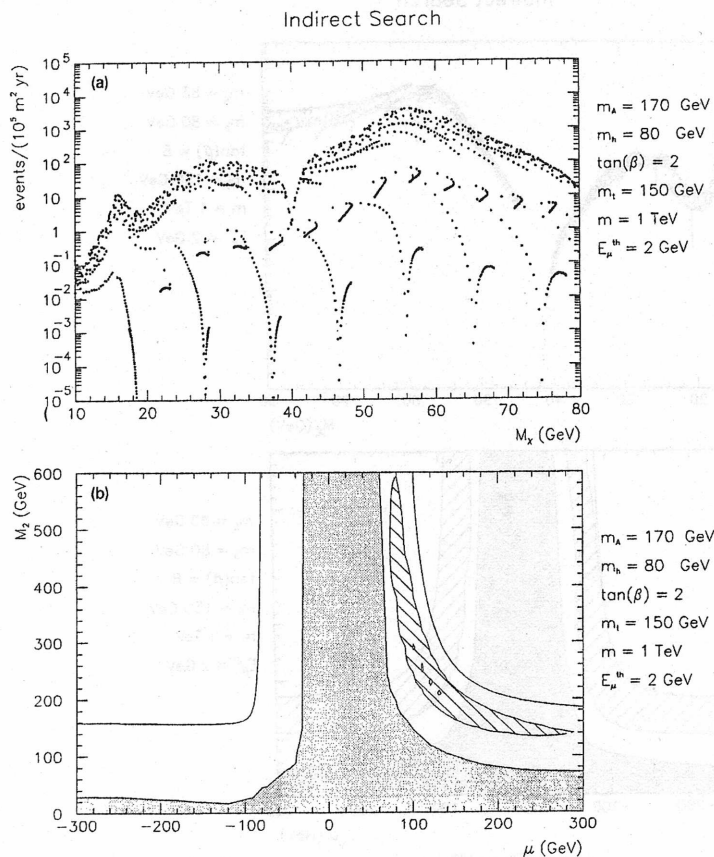
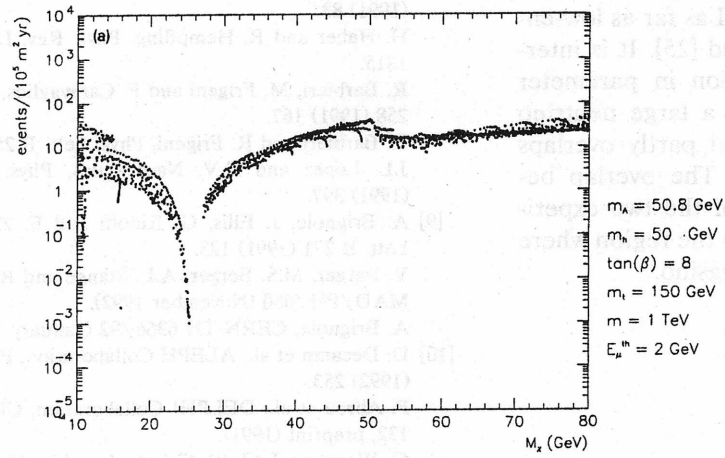


Figure 12b

Fig. 12. Same as in fig. 11 with $\tan \beta = 2$, $m_\chi = 80$ GeV, $m_A = 170$ GeV.

Indirect Search – Sun



Indirect Search – Sun

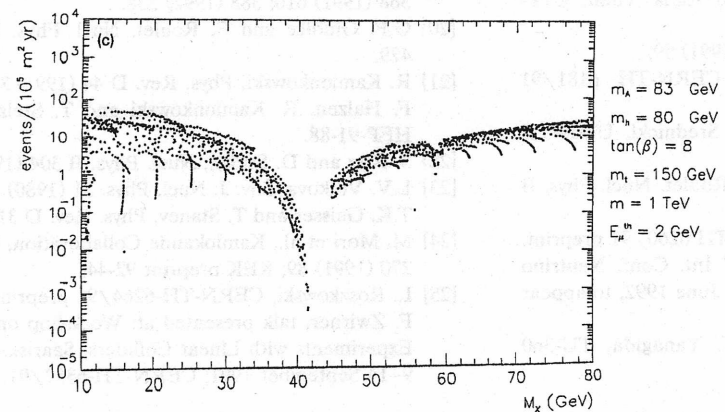
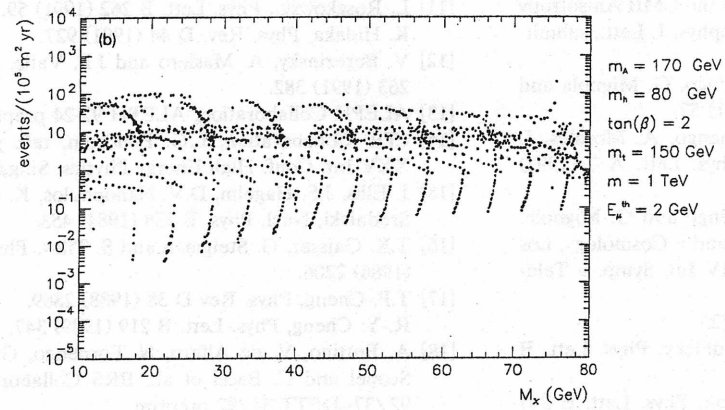


Fig. 13. Indirect detection of neutralinos ($\chi\chi$ annihilation in the Sun): rates of outgoing muons per year in a detector of area 10^5 m^2 as a function of m_χ . Half aperture is taken 25° . ρ_χ is rescaled. The threshold for muons is 2 GeV. (a) $\tan \beta = 8$, $m_h = 50 \text{ GeV}$, $m_A = 50.8 \text{ GeV}$; (b) $\tan \beta = 2$, $m_h = 80 \text{ GeV}$, $m_A = 170 \text{ GeV}$; (c) $\tan \beta = 8$, $m_h = 80 \text{ GeV}$, $m_A = 83 \text{ GeV}$.

There have been recent investigations about the discovery potential at LEP II as far as low-energy supersymmetry is concerned [25]. It is interesting to remark that the region in parameter space that can be explored by a large neutrino telescope is complementary and partly overlaps the one accessible at LEP II. The overlap between the sensitivity domains of the two experimental searches concerns mainly the region where the neutralino is dominantly higgsino.

References

- [1] G.F. Smoot et al., Structure in the COBE DMR First Year Maps, *Astrophys. J. Lett.*, submitted (April 1992).
- [2] E.L. Wright et al., Interpretation of the CMB Anisotropy detected by the COBE DMR, *Astrophys. J. Lett.*, submitted (April 1992).
- [3] A. Bottino, V. de Alfaro, N. Fornengo, G. Mignola and M. Pignone, *Phys. Lett. B* 265 (1991) 57.
A. Bottino, V. de Alfaro, N. Fornengo, A. Morales, J. Puimedón and S. Scopel, *Mod. Phys. Lett. A* 7 (1992) 733; *Proc. TAUP91*.
A. Bottino, V. de Alfaro, N. Fornengo and G. Mignola, in: *Proc. II UCLA Int. Conf. γ -ray and ν Cosmology*, Los Angeles, February 1992; in: *Proc. IV Int. Symp. ν Telescopes*, Venezia, March 1992.
- [4] P. Fayet, *Phys. Lett. B* 86 (1979) 272.
R. Flores, H.A. Olive and M. Srednicki, *Phys. Lett. B* 237 (1990) 72.
J. Ellis, L. Roszkowski and Z. Lalak, *Phys. Lett. B* 245 (1990) 545.
J.L. Lopez, D.V. Nanopoulos and Kajia Yuan, *CTP-TAMU-31/91 preprint*.
L. Roszkowski, *Phys. Lett. B* 262 (1991) 59.
K. Griest and L. Roszkowski, *CERN-TH 6181/91 preprint*.
J. McDonald, H.A. Olive and M. Srednicki, *UMN-TH 1017/92 preprint*.
- [5] G.B. Gelmini, P. Gondolo and E. Roulet, *Nucl. Phys. B* 351 (1991) 623.
- [6] J. Ellis and L. Roszkowski, *CERN-TH 6260/91 preprint*.
- [7] V. Berezinsky, invited talk at: *XV Int. Conf. Neutrino Physics and Astrophysics*, Granada, June 1992, to appear in *Nucl. Phys. Suppl.*
- [8] Y. Okada, M. Yamaguchi and T. Yanagida, *TU-360 preprint* (1990).
- J. Ellis, G. Ridolfi and F. Zwirner, *Phys. Lett. B* 257 (1991) 83.
- H. Haber and R. Hempfling, *Phys. Rev. Lett.* 66 (1991) 1815.
- R. Barbieri, M. Frigeni and F. Caravaglios, *Phys. Lett. B* 258 (1991) 167.
- R. Barbieri and R. Frigeni, *Phys. Lett. B* 258 (1991) 395.
- J.L. Lopez and D.V. Nanopoulos, *Phys. Lett. B* 266 (1991) 397.
- [9] A. Brignole, J. Ellis, G. Ridolfi and F. Zwirner, *Phys. Lett. B* 271 (1991) 123.
V. Barger, M.S. Berger, A.L. Stange and R.J.N. Phillips, *MAD/PH/680* (November 1992).
A. Brignole, *CERN-TH-6366/92* (January 1991).
- [10] D. Decamp et al., *ALEPH Collaboration*, *Phys. Rep.* 216 (1992) 253.
P. Abreu et al., *DELPHI Collaboration*, *CERN-PPE-91-132*, preprint (1991).
G. Wormser, *LAL 91-47 Lab. Acc. Lin. Orsay*, (October 1991); invited talk at: *Int. Meeting on Elementary Particle Physics*, Kazimierz, Poland, 27–31 May 1991.
- [11] L. Roszkowski, *Phys. Lett. B* 262 (1991) 59.
K. Hidaka, *Phys. Rev. D* 44 (1991) 927.
- [12] V. Berezinsky, A. Masiero and J.F. Valle, *Phys. Lett. B* 263 (1991) 382.
- [13] *ALEPH Collaboration*, *ALEPH 92-24 preprint*.
- [14] *CDF Collaboration*, L.G. Pondrom, talk presented at: *XXV Int. Conf. High Energy Physics*, Singapore 1990.
- [15] J. Ellis, J.S. Hagelin, D.V. Nanopoulos, K. Olive and M. Srednicki, *Nucl. Phys. B* 238 (1984) 453.
- [16] T.K. Gaisser, G. Steigman and S. Tilav, *Phys. Rev. D* 34 (1986) 2206.
- [17] T.P. Cheng, *Phys. Rev. D* 38 (1988) 2869.
R.-Y. Cheng, *Phys. Lett. B* 219 (1989) 347.
- [18] A. Bottino, V. de Alfaro, N. Fornengo, G. Mignola, S. Scopel and C. Bacci et al., *BRS Collaboration*, *LNGS 92/37-DFTT 34/92 preprint*.
- [19] A. Gould, *Astrophys. J.* 321 (1987) 571; 328 (1988) 919; 368 (1991) 610; 388 (1992) 338.
- [20] G.F. Giudice and E. Roulet, *Nucl. Phys. B* 310 (1989) 429.
- [21] R. Kamionkowski, *Phys. Rev. D* 44 (1991) 3021.
F. Halzen, R. Kamionkowski and T. Stelzer, *IASSNS-HEP-91-88*.
- [22] S. Ritz and D. Seckel, *Nucl. Phys. B* 304 (1988) 877.
- [23] L.V. Volkova, *Sov. J. Nucl. Phys.* 31 (1980) 784.
T.K. Gaisser and T. Stanev, *Phys. Rev. D* 31 (1985) 2770.
- [24] M. Mori et al., *Kamiokande Collaboration*, *Phys. Lett. B* 270 (1991) 89; *KEK preprint 92-44*.
- [25] L. Roszkowski, *CERN-TH-6264/91 preprint* (1991).
F. Zwirner, talk presented at: *Workshop on Physics and Experiments with Linear Colliders*, Saariselkä, Finland, 9–14 September 1991; *CERN-TH-6357/91*.